AIMS Microbiology

AIMS Microbiology, 12(4): 789–814.
DOI: 10.3934/microbiol.2026034
Received: 13 August 2026
Revised: 07 October 2026
Accepted: 19 October 2026
Published: 30 October 2026

https://www.aimspress.com/journal/microbiology

Research article

Probiotic biogenics-mediated augmentation of phage therapy against multidrug-resistant Enterotoxigenic *Escherichia coli*

Abishek Mani[1], Nashath Kalangadan[1], Sharayu Magar[2], Barath Sivaraj[2], Gospel Gabriel Xavier[1], Thirumalai Diraviyam[3], Srivignesh Sundaresan[4], Sutharsan Govindarajan[2] and Kaushik Rajaram[1,*]

[1] Department of Microbiology, Central University of Tamil Nadu, Thiruvarur-610005, Tamil Nadu, India
[2] Department of Biological Sciences, SRM University, AP, Amaravati-522240, Andhra Pradesh, India
[3] Centre for Research in Infectious Diseases (CRID), Department of Bioengineering, School of Chemical & Biotechnology, SASTRA Deemed-to-be-University, Thanjavur-613401, Tamil Nadu, India
[4] Department of Horticulture, Central University of Tamil Nadu, Thiruvarur-610005, Tamil Nadu, India

* **Correspondence:** Email: rkaushik@cutn.ac.in; Tel: +914366277230.

Abstract: Enterotoxigenic *Escherichia coli* (ETEC) is one of the most common causative agents of foodborne gastroenteritis globally, spreading through contaminated water and food. The rising incidence of multidrug-resistant (MDR) bacteria has produced an urgent need for alternative antimicrobial treatments. Bacteriophages are potential therapeutic agents against MDR infections; yet, the development of phage resistance remains a critical limitation to their clinical applications. In this study, we isolated and characterized an ETEC-targeting lytic bacteriophage (CU10EC) with potent antibacterial activity. Phage resistance was observed within ~10 h of treatment, making phage therapy ineffective. To address this limitation, we used a novel combinatorial approach that combined cell free probiotic biogenics (PB) produced by the probiotic bacterium *Lactobacillus acidophilus* with CU10EC-mediated therapy. The PB contains a rich array of biomedically relevant components, including organic acids, antimicrobial peptides, short-chain fatty acids, and proteolytic enzymes, as confirmed by LC-MS analysis. It demonstrated effective antibacterial activity against MDR-ETEC, broad-spectrum activity against other pathogens, and less or no antibacterial activity against commensals. Importantly, in the presence of phage CU10EC, only two-thirds of the PB concentration was required for complete bacterial killing. Additionally, the consecutive administration of PB at 2, 4, and 6 h in a time-kill assay delayed phage resistance by 6–10 h. Overall, the CU10EC-PB combination offers a novel method to enhance antibacterial activity, while conserving gut commensals and delaying phage resistance.

Keywords: Enterotoxigenic *Escherichia coli*; bacteriophage therapy; phage combination; foodborne pathogen; gut health; phage stability

1. Introduction

Enterotoxigenic *Escherichia coli* (ETEC) is a leading cause of enteric diseases and traveler's diarrhea, particularly among children and older adults. It is estimated to cause 18,700–42,000 deaths annually in low- and middle-income countries [1,2]. In addition to poor hygiene conditions and contaminated water, meat, cereals, and vegetables are the main sources of ETEC contamination [3]. Symptoms, including watery diarrhea that may lead to severe dehydration, typically appear within 8–72 h after ingestion of contaminated food or water. For ETEC infections, the primary therapeutic approach is oral rehydration, which can restore the fluid and electrolyte balance [4]. Antibiotics may be prescribed depending on the severity of the case, such as prolonged dehydration, persistent high fever, or traveler's diarrhea [5]. The inappropriate use of antibiotics for enteric infections has further accelerated the emergence and spread of antimicrobial resistance (AMR) [6]. Historically, ETEC was susceptible to most conventional antibiotics. However, the widespread emergence of AMR has resulted in ETEC strains resistant to multiple antibiotic classes, including cephalosporins, β-lactams, tetracyclines, sulfonamides, aminopenicillins, macrolides, and fluoroquinolones [7,8].

Phages are the most abundant biological entities in nature and offer highly specific antibacterial activity against their target bacteria, enabling the treatment of multidrug-resistant (MDR) infections with minimal disruption to the normal gut microbiota [9–11]. Phage therapy has emerged as a promising strategy for controlling ETEC infections, which are associated with significant morbidity, mortality, and economic burden worldwide [12,13]. Phage resistance is an evolutionary survival strategy in bacteria that enables them to evade phage predation. Bacteria develop resistance to phages at various stages of phage infection, ranging from cell-surface modifications that counter phages to defense systems such as restriction-modification or the CRISPR-Cas adaptive immune mechanism [14].

In the context of phage therapy, the rapid emergence of phage-resistant variants remains a major challenge. This challenge is commonly addressed using phage cocktails composed of multiple phages that recognize different bacterial receptors. A recent study reported that a five-phage cocktail against vancomycin-resistant *Enterococcus* (VRE) induced only a minimal inflammatory response in a mouse model. However, the host anti-phage immune response was found to reduce the therapeutic efficacy of phage treatment [15]. Additionally, the cocktail of phages must not encode AMR genes, virulence factors, or toxins [16]. These factors make the use of cocktails more complex and demanding in clinical applications. Phage-antibiotic combination therapy is a promising approach to limit phage resistance in MDR pathogens while helping to understand the selective pressures that drive antibiotic resistance [17,18]. Combining phages with alternative antimicrobials such as nanoparticles, antimicrobial peptides (AMPs), antibodies, and postbiotics may promote phage efficacy and help overcome therapeutic limitations. Among the above, postbiotics have gained attention due to their antimicrobial activity, stability, safety, and cost-effectiveness. Furthermore, postbiotics were reported not to induce any antimicrobial resistance in the pathogens [19].

Probiotic biogenics (PB) are cell-free preparations of probiotics that contain bioactive metabolites produced by probiotic microorganisms and can be referred to as cell-free postbiotics. These types of postbiotics, or PBs, lack inanimate cells and their components, which may reduce immune responses

to the PB [20]. These preparations contain metabolites such as organic acids, short-chain fatty acids, enzymes, and antimicrobial peptides that contribute to their antimicrobial, antioxidant, anti-inflammatory, and other beneficial biological activities [21]. PBs have been reported to help maintain gut microbial homeostasis, modulate immune responses, and influence host gene expression [22,23]. Compared with live probiotics, PBs offer several practical advantages, including improved storage stability, ease of transportation, no risk of transferring antimicrobial resistance genes, and easier incorporation into food products [24]. A recent study reported that the PB-antibiotic combination enhanced their efficacy against nosocomial pathogens, demonstrating promising synergistic activity [25].

We hypothesize that the combination of a lytic bacteriophage with a PB is expected to enhance antibacterial activity against MDR ETEC, as PBs are rich in organic acids and antimicrobial peptides that can destabilize the bacterial membranes and lower the pH, thereby weakening the ETEC cells. This membrane damage could facilitate phage CU10EC infection and delay the formation of phage resistance. In this study, we isolated and characterized a novel lytic bacteriophage (CU10EC) targeting MDR ETEC and investigated its antibacterial activity. We also evaluated the antibacterial activity of a cell-free PB derived from *Lactobacillus acidophilus* against MDR pathogens and assessed its selectivity for pathogenic and representative commensal bacteria. We further investigated whether combining the PB with phage CU10EC could enhance antibacterial efficacy and delay the emergence of phage-resistant bacteria.

2. Materials and methods

2.1. Phage isolation and characterization

2.1.1. Isolation and purification of phage

Samples were collected directly from sewage water and soil near the sewage area in and around Central University of Tamil Nadu (CUTN), located in Thiruvarur, Tamil Nadu, India.

For processing, ~10 mL of liquid sewage was added to 30 mL of sterile phage buffer (SM buffer) in a 50 mL centrifuge tube. In the case of soil samples, 10 g of soil was mixed in 30 mL of phage buffer. The mixtures were incubated undisturbed at room temperature for 24 h. Post-incubation, samples were centrifuged at 10,000 rpm, and the supernatant was filtered through a 0.22 µm syringe filter to remove debris and bacteria. For enrichment, 1 mL of the overnight ETEC (MTCC 723) culture was added to 3 mL of the filtered sample, along with sterile Luria Bertani (LB) broth, to a final volume of 10 mL. This mixture was incubated at 37 ℃ with shaking (~125 rpm) for 18–24 h. After enrichment, samples were centrifuged at 10,000 rpm for 10 min, and the supernatant was filter-sterilized using a 0.22 µm syringe filter. The phage lysate was serially diluted to 10^{-6} PFU/mL. A 50 µL volume of phage lysate from each dilution was mixed with 200 µL of ETEC culture, incubated for 10–15 min, and combined with 0.7% top agar. The mixture was poured onto LB agar plates containing 2% agar and incubated for 24 h at 37 ℃. Plaques were selected using sterile tips and placed in a microtiter plate containing 100 µL of phage buffer. These were then serially diluted and plated in the same manner until a uniform plaque morphology was obtained.

2.1.2. Phage amplification and titration

Phage amplification was carried out by adding phage buffer to a plate containing plaques with uniform morphology. The plate was kept at 4 ℃ for 24 h to allow phage diffusion into the buffer. Following incubation, the phage buffer was collected and enriched by mixing it with an overnight-grown ETEC culture in LB broth, using the same enrichment ratio as previously. Post 18–24 h of incubation at 37 ℃ with shaking, the lysate was centrifuged and sterilized with a 0.22 μm syringe filter, as previously stated. The purified phage lysate was then serially diluted up to 10^{-12}. From each dilution, 3 μL of phage lysate was spotted onto a bacterial lawn composed of LB top agar pre-mixed with 200 μL of an overnight ETEC culture. The spotted plates were allowed to air-dry briefly and were incubated overnight at 37 ℃. Post-incubation, phage titer was calculated by manually counting the plaques from the corresponding dilution on the plates.

2.1.3. Transmission electron microscope (TEM) imaging of phage

TEM analysis was carried out to determine the size and shape of the phage. An enriched phage lysate was prepared for TEM imaging, and ~10 μL of the lysate was placed on a 200-mesh carbon film grid and allowed to air-dry; excess phage lysate was wiped away using Kimwipes. The absorbed phage on the grid was negatively stained with uranyl acetate (Electron Microscopy Sciences). Then, the phage-absorbed carbon grid was imaged using a JEOL 2100 Plus electron microscope at 200 kV. The morphology of the phage was examined and measured as previously described [26].

2.1.4. Sequencing and genome analysis of phage

Genomic libraries were prepared using the KAPA DNA Hyper Prep kit and sequenced on a NovaSeq X Plus platform (2 × 151 bp), generating a total output of 3.7–4.3 GB with 100 × coverage. Read quality was assessed using FastQC (v0.11.8) (https://www.bioinformatics.babraham.ac.uk/projects/fastqc/), and low-quality bases and adapter sequences were removed using Trim Galore (v0.4.3) (https://github.com/FelixKrueger/TrimGalore). The resulting high-quality reads were assembled de novo with SPAdes (v3.1.1) [27] via the Galaxy CPT server. Assembly quality and genome completeness were assessed using PhageScope [28]. Genome annotation were performed with Pharokka [29], while the DNA type prediction was confirmed using Pharokka and Bandage (v2022.09) [30]. The phage life cycle was inferred using PhaTYP [31]. Taxonomic classification was carried out using Taxmyphage [32], using the genome database available as of August, 2025. The phage genome was visualized both as a linear map using Linear Genome Plot [33] and as a circular map using Snapview (https://www.snapgene.com/snapgene-viewer). Comparative genomic analysis was conducted with ViPTree [34], using the genome database available as of August, 2025, aligning the phage genome to related sequences and generating a proteomic tree based on tBLASTx similarities. Both circular and rectangular phylogenetic trees were created for visualization using VipTree. Antimicrobial-resistance and virulence-associated genes were screened using PhageScope.

2.1.5. Phage host range

The host range of CU10EC was analyzed using an adapted method from Wang et al. [35]. Initially, susceptible bacterial strains were screened using a spot assay, and quantitative host range efficacy was determined by efficiency of plating (EOP). CU10EC and screened bacterial cultures (Table 1) were mixed and plated using the agar overlay method. After overnight incubation at 37 ℃, the plaques were observed and counted. The EOP values were determined as the ratio of PFUs of phage-susceptible strains to PFUs calculated for ETEC.

Table 1. Host range of CU10EC and efficiency of plating.

No	Bacterial strains	Efficiency of plating (EOP) value
1.	ETEC MTCC 723 (host)	1
2.	*E. coli* (MG1655)	0.0208 ± 0.0033
3.	*E. coli* (TG1)	0.0147 ± 0.0067
4.	*E. coli* (ATCC 25922)	–
5.	*E. coli* (MCC 2246)	–
6.	*E. coli* (ATCC 11775)	–
7.	*E. coli* (DH5α)	–
8.	*Uropathogenic E. coli* (UPEC) (MTCC 729)	–

*Note: Phage-insensitive mutants are denoted as "–" in the table. Data were plotted as mean ± standard deviation (SD) values of replicates (n = 3).

2.1.6. Phage adsorption studies

Phage adsorption studies were conducted using a previously established protocol [26] with modifications. Bacteria and CU10EC were mixed at a multiplicity of infection (MOI) of 1 by combining 100 µL of a 0.5 McFarland standard bacterial suspension with 100 µL of phage, and the volume was adjusted to 1 mL using nutrient broth (NB). As a control, 100 µL of phage was mixed with 900 µL of NB to determine the total phage count. The mixtures were incubated in a shaking incubator at 37 ℃ for 10 min, followed by 5 min at room temperature. After incubation, the samples were centrifuged at 10,000 rpm for 10 min. From the supernatant, 10 µL was serially diluted and spotted on the double agar overlay to determine the concentration of free phage.

2.1.7. One-step growth curve

The one-step growth curve assay of CU10EC was adapted from Hu et al.'s protocol [36]. 100 µL of bacteria (10^7 CFU) and 100 µL of phage (10^7 PFU) were added to 800 µL of NB to obtain a 1 MOI, and the mixture was incubated at 37 ℃ at 180 rpm for 10 min. After incubation, the tubes were

centrifuged at 10,000 rpm for 1 min, and the supernatant was removed. The remaining pellet was washed with fresh medium, and the washing process was repeated twice. The sample was incubated at 37 ℃ with a rotation speed of 180 rpm. Every 10 min, starting from the 0th minute, 10 μL of sample was taken after centrifugation at 10,000 rpm for 1 min. A 10 μL supernatant was ten-fold serially diluted in a microtiter plate and spotted onto an agar overlay to determine the phage titer. The burst size was calculated using the following formula: Phage titer at plateau-initial phage titer/initial cell density [37,38].

2.1.8. Multiplicity of infection (MOI) determination

MOI is a crucial phenomenon to understand phage-bacterial interactions. Bacteria were grown overnight and standardized to the required CFU/mL using the McFarland standard method. The phage CU10EC was also prepared at different titers to obtain a range of MOIs. The exact number of bacteria (~10^5 CFU/mL) was mixed with phages at varying titers to achieve MOIs of 0.0001, 0.001, 0.01, 0.1, 1, 10, 100, and 1000. All these mixtures of different MOIs were prepared in a 96-well plate and incubated at 37 ℃ at 100 rpm for 24 h. Bacterial growth at different MOIs was analyzed by measuring absorbance at 600 nm using a GloMax® Discover Microplate Reader (Promega Corporation, USA) at 2-h intervals starting at the 0th hour.

2.1.9. Phage stability assays

The thermal and pH stability of the phage was assessed using established protocols from previous ETEC phage studies [36,39]. For both assays, 100 μL of the enriched phage lysate (CU10EC) was mixed with 900 μL of phage buffer to achieve a final volume of 1 mL per sample. For thermal stability, the phage samples were incubated at various temperatures (4, 10, 20, 30, 40, 50, 60, 70, and 80 ℃) for 4 h. To assess pH stability, 9 mL of phage buffer in separate tubes was adjusted to different pH levels (pH 3, 5, 7, 9, and 11), and 1 mL of phage was incubated at 37 ℃ for 4 h. Following incubation, the phage titer was determined using the double agar overlay spot method. The stability of CU10EC was assessed in the presence of bile salt at different concentrations using the double agar overlay spot method. The bile salt was prepared at concentrations of 2%, 1%, and 0.5% in sterile centrifuge tubes. 100 μL of CU10EC (~10^7 PFU/mL) was added to the various concentrations of bile salts and with control (900 μL of water) in centrifuge tubes to a total volume of 1 mL, and the titer of the phage was assessed every hour, from the 0th to the 3rd hour, to observe the stability of the phage in the presence of bile salt at 37 ℃ incubation at ~100 rpm.

2.2. Comparative analysis of wild-type (WT) and phage-resistant (PR) ETEC

2.2.1. Phenotypic modification in WT-ETEC and PR-ETEC

The PR-ETEC strain was isolated using a serial phage-exposure method in liquid co-culture, followed by subculturing to ensure purity. To completely eliminate any residual carrying phage particles, the cultured cells were subjected to multiple rounds of centrifugation (3 rounds at 10,000 rpm for 10 min) in sterile PBS. Then, bacteria were plated on nutrient agar to obtain individual colonies. The overnight culture from the bacteriophage-insensitive mutant (BIM) was used to determine the resistant phenotype by the agar overlay method and the kinetic growth curve assay. The phenotypic

modifications were compared between WT-ETEC and PR-ETEC, using two methods. In the first method, both WT-ETEC and PR-ETEC strains were grown to reach up to 0.5 OD. 10 µL of each bacterial culture was added to 190 µL of LB broth in a microtiter plate and incubated at 37 ℃ with continuous shaking at 100 rpm. Growth was analyzed by measuring absorbance at 600 nm every 2 h for a total duration of 12 h using the GloMax® Discover Microplate Reader (Promega Corporation, USA). In the second method, colony morphology and growth patterns were observed by adding 5 µL of WT-ETEC and PR-ETEC at a 10 mm distance on the surface of an LB agar plate, and the plate was incubated at 37 ℃ for 48 h.

2.2.2. Antibiogram of WT-ETEC and PR-ETEC

Antibiotic susceptibility profiles of the ETEC-WT and ETEC-PR strains were evaluated using the disk diffusion method in accordance with the Clinical and Laboratory Standards Institute (CLSI) M100 guidelines [40]. *Escherichia coli* ATCC 25922 was utilized as the quality-control reference strain. A total of 23 antibiotics were tested, including DO 30 (Doxycycline, 30 µg), AK 30 (Amikacin, 30 µg), S 10 (Streptomycin, 10 µg), TOB 10 (Tobramycin, 10 µg), TE 30 (Tetracycline, 30 µg), GEN 10 (Gentamicin, 10 µg), MRP 10 (Meropenem, 10 µg), IPM 10 (Imipenem, 10 µg), C 30 (Chloramphenicol, 30 µg), E 15 (Erythromycin, 15 µg), LE 5 (Levofloxacin, 5 µg), CFM 5 (Cefixime, 5 µg), OF 5 (Ofloxacin, 5 µg), VA 30 (Vancomycin, 30 µg), RIF 5 (Rifampin, 5 µg), CD 2 (Clindamycin, 2 µg), CPD 10 (Cefpodoxime, 10 µg), MET 5 (Methicillin, 5 µg), AMX 10 (Amoxicillin, 10 µg), P 10 (Penicillin G, 10 µg), AMP 10 (Ampicillin, 10 µg), NX 10 (Norfloxacin, 10 µg), and NAF 1 (Nafcillin, 1 µg). Bacterial lawn on the Mueller-Hinton Agar (MHA) plates were prepared by uniformly spreading 250 µL of each bacterial strain using sterile cotton swabs. Antibiotic discs were placed on the bacterial lawn using sterile forceps, and the plates were incubated at 37 ℃ overnight. Zones of inhibition were measured to determine the antibiotic susceptibility of each strain.

2.2.3. Assessing the biofilm-forming ability of WT-ETEC and PR-ETEC in the Congo Red Agar plate method and crystal violet assay

The Congo Red Agar (CRA) method was used to assess biofilm formation in WT-ETEC and PR-ETEC. Overnight cultures were standardized to 0.5 McFarland, and CRA plates were prepared with 3.6% brain heart infusion (BHI) broth, 5.3% sucrose, 1% agar, and 0.8% Congo Red (added post-autoclaving) [41]. Cultures of WT-ETEC and PR-ETEC were streaked onto the plates, which were incubated at 37 ℃ for 24 h to compare biofilm-forming patterns. Both WT-ETEC and PR-ETEC strains were tested for quantitative biofilm formation using the crystal violet assay. In a 96-well plate, 10 µL of bacterial cultures (~1.5×10^6 CFU/mL) were inoculated into a well containing 190 µL of BHI medium, and 200 µL of medium alone was kept as a control; the plate was incubated for 24 h at 37 ℃ in a shaking incubator at ~100 rpm. Post-incubation, the planktonic cells of WT-ETEC and PR-ETEC were aspirated from the wells and washed twice with PBS. After the washing step, 100 µL of 0.1% crystal violet was added to the wells and incubated for 30 min at room temperature. Then, crystal violet was removed from each well, and the wells were washed again with PBS. The washed wells were allowed to dry at room temperature. Then, 200 µL of 100% ethanol was added to each well and mixed well by pipetting. Then, the mixed solution was transferred to a new 96-well plate for absorbance reading at 600 nm.

2.3. Preparation and characterization of PB

2.3.1. Media optimization

Probiotics, such as *Lactobacillus*, require specific growth media, like De Man-Rogosa-Sharpe (MRS) broth, for optimal growth. Modified growth medium was developed to support the growth of both ETEC and *Lactobacillus* species. The base medium was prepared by dissolving 1% tryptone, 0.5% yeast extract, 0.5% sodium acetate, 0.1% polysorbate (Tween 80), 0.01% magnesium sulfate, 0.2% di-potassium hydrogen phosphate, and 1% sodium chloride in distilled water, followed by sterilization through autoclaving. After sterilization, sterile 1.5% dextrose (filter-sterilized) was added to the medium, and the pH was determined to be ~7.2 (± 0.2) before use.

2.3.2. PB production and screening

An overnight culture of *L. acidophilus* (MTCC-10307) was prepared and standardized to a 0.5 McFarland standard (~1.5×10^8 CFU/mL). Subsequently, 1 mL of the 0.5 McFarland bacterial preparation was inoculated into 19 mL of modified medium at pH 7.2 (± 0.2). The culture was then incubated at 37 ℃ for 48 h in a shaking incubator at ~125 rpm. Following incubation, the culture was centrifuged at 10,000 rpm for 5 min to obtain a cell-free PB. These PBs were sterilized with 0.22 μM syringe-driven filters and refrigerated for further experimental analysis. Following sterilization/preparation, the PB was heated at 80 ℃ for 1 h. This step was carried out to selectively denature and inactivate heat-labile macromolecular fractions, such as proteolytic enzymes, to minimize proteolytic activity that could affect the phage stability in the combination.

2.3.3. Liquid Chromatography-Mass Spectroscopy (LC-MS) analysis of PB

LC-MS analysis of the PB was performed to determine the presence of small organic acids, short-chain lipids, and peptide-range bioactive compounds. The cell-free supernatant was filtered (0.22 μM) and analyzed on a Waters XBridge C18 column (4.6 × 150 mM, 5 μM) using a 10-min gradient of 0.05% formic acid in water (A) and acetonitrile (B) at 0.4 mL/min. Electrospray ionization was employed in both positive (ESI+) and negative (ESI−) modes on a Q-TOF mass spectrometer with full-scan acquisition (m/z 50–2000) and stepped collision energies (20/35/50 eV) for MS/MS fragmentation. Data were processed using MZmine 3 for peak detection, alignment, and deconvolution. Background chemical noise from the modified medium was removed using an automated Blank Filtering workflow, excluding features with an ion-intensity fold change < 5.0 relative to the sterile media blank. Compound identification confidence followed strict Metabolomics Standards Initiative (MSI) guidelines: Level 1 (authentic standards), Level 2 (exact mass and library match), Level 3 (tentative compound class), and Level 4 (unidentified features characterized by exact m/z and retention time).

2.3.4. Well diffusion plate method

An overnight ETEC culture was prepared, and 100 μL of the culture was spread onto MHA plates to form a uniform bacterial lawn. Wells were carefully made on the plates using sterile cork borers of

two different sizes. Subsequently, 100 µL and 50 µL of PB were dispensed into the respective wells. The plates were then incubated at 37 ℃ for 24 h.

2.3.5. Minimum inhibitory concentration of PB

An overnight ETEC culture was prepared and standardized as a 0.5 McFarland standard. In a sterile, non-tissue culture-treated microtiter plate, 10^6 CFU of ETEC was inoculated into each well, and PB was added to the modified medium at different ratios. The volume of PB added to each well was 50%, 45%, 40%, 35%, 30%, 25%, 20%, 15%, 10%, and 5%; the wells were then made up to 200 µL with modified medium. 10^6 CFU of bacteria was added to the modified medium as a control, and media without bacteria were maintained as blank controls. After adding samples to the microtiter plate, the plate was incubated for 24 h at 37 ℃ in a shaking incubator at ~100 rpm.

2.3.6. Poison plate method

Bacterial agar plates were prepared by mixing antimicrobial agents with the bacterial growth media, called poison plates. 25% of sterile *L. acidophilus*-based PB (LA-PB) and *L. plantarum*-PB (LP-PB) were mixed with the autoclaved LB agar. Pathogenic bacteria, including ETEC, *Pseudomonas aeruginosa* (ATCC-15442), *Staphylococcus aureus* (ATCC-25923), *Enterococcus faecalis* (ATCC-14506), and *Achromobacter spp.* (WT), were streaked onto PB plates and LB agar plates as a control for comparison. Post-inoculation plates were incubated at 37 ℃ overnight.

2.3.7. Antibacterial selectivity of PB

The antibacterial efficacy of PB was evaluated against probiotic bacteria using the serial micro broth dilution method. In a sterile 96-well plate, 0.5 McFarland standards of *L. plantarum* (MTCC-1407), *L. spp.* (MTCC-4184), *L. brevis* (MTCC-1750), *L. acidophilus* (MTCC-10307), and *L. salivarius* (MTCC-12829), cultures were prepared and 10^6 CFU added to each well along with 40%, 35%, 30%, 25%, 20%, 15%, 10%, and 5% of PB in the modified media, which was made up to 200 µL. The plate was incubated at 37 ℃ in a shaker incubator at ~100 rpm for 24 h.

2.4. Phage-PB combination studies

2.4.1. Checkerboard assay

A checkerboard assay was performed to evaluate the optimal combination of phage MOI and PB concentration. In a sterile 96-well plate, PB concentrations ranging from 35% to 5% were tested against phage MOIs of 10, 1, and 0.1, with a constant bacterial load of 10^6 CFU per well. Phage dilutions were adjusted accordingly to achieve the desired MOIs. The microtiter plate was incubated in a shaker incubator at ~100 rpm and 37 ℃. Post-incubation, the absorbance was measured at 600 nm using the GloMax® Discover Microplate Reader (Promega Corporation, USA).

2.4.2. Time-dependent kinetics curve assay

A time-dependent kinetics curve assay was conducted to assess the delay in phage resistance and biomass reduction during phage-PB combination therapy. The PB was added at four time points (0, 2, 4, and 6 h) during a 24-h study period with the phage at an MOI of 1 and PB concentrations ranging from 35% to 5%. Bacterial growth was monitored every 2 h by measuring absorbance at 600 nm using the GloMax® Discover Microplate Reader (Promega Corporation, USA). The microtiter plate was incubated at 37 ℃ in a shaking incubator at ~100 rpm. The experiments were conducted in triplicate.

2.5. Statistical analysis

All quantitative assays were performed with independent biological replicates, each containing a minimum of three technical replicates. Data are expressed as mean ± standard deviation (SD), and were analyzed using GraphPad Prism 8.3. End-point parameters were evaluated using standard one-way or two-way ANOVA. To account for within-experiment correlation in repeated time-course kinetic data, repeated measures (RM) two-way ANOVA with a Greenhouse-Geisser correction was applied. Post-hoc group comparisons were resolved using Tukey's test to control the family-wise error rate. Statistical significance was defined at $p < 0.05$ (ns: non-significant; * $p \leq 0.05$; ** $p \leq 0.01$; *** $p \leq 0.005$; **** $p \leq 0.0001$).

3. Results

3.1. Isolation and TEM analysis of ETEC bacteriophage

ETEC (MTCC 723) was used to isolate phages from the collected sewage samples. Plaques with distinct morphologies were observed. One plaque was predominant, measuring ~2 ± 0.2 mm with an extending hollow zone (Figure 1A). This plaque was purified by repeated plating and further enriched to a titer of ~1.3 × 10^8 PFU/mL, and the phage was named as *E. coli* phage *vB_EcoP*_CU10EC. TEM images of CU10EC showed an icosahedral head with a diameter of ~67 nm and a non-contractile tail fiber, resembling *podovirus* morphology (Figure 1B). Based on these features, CU10EC was classified under the order Caudovirales.

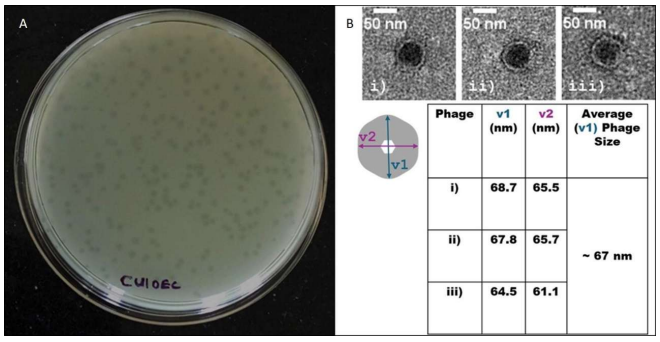


Figure 1. Phage morphological identification. (A) Plate with distinctive plaque morphology for CU10EC; (B) TEM images of CU10EC with the size scale and average phage size in nm.

3.2. Genome analysis of ETEC phage CU10EC

Whole-genome sequencing of the isolated *Escherichia* phage CU10EC revealed a genome size of 73,004 bp, with an average GC content of 42.54% and a coding density of 95.38%. The complete genome sequence of CU10EC has been deposited in GenBank under accession number PQ435408, and the phage was designated as vB_EcoP_CU10EC in accordance to the ICTV recommendations for phage nomenclature. PhageScope analysis confirmed that the CU10EC was a complete genome (Figure S1). Additionally, Pharokka and Bandage analysis verified that the genomic DNA of CU10EC was linear. Pharokka annotation also identified 112 protein-coding open reading frames (ORFs) along with two transfer RNAs (tRNAs). Functional annotation identified genes encoding phage holin (XKC24791.1) and endolysin (XKC24792.1). Of the 112 ORFs, 31 were assigned putative functions, while the remaining 81 were classified as hypothetical proteins (Figure 2A,B). No genes associated with antimicrobial resistance or virulence were detected (Figure S2), indicating that the isolated phage has therapeutic potential.

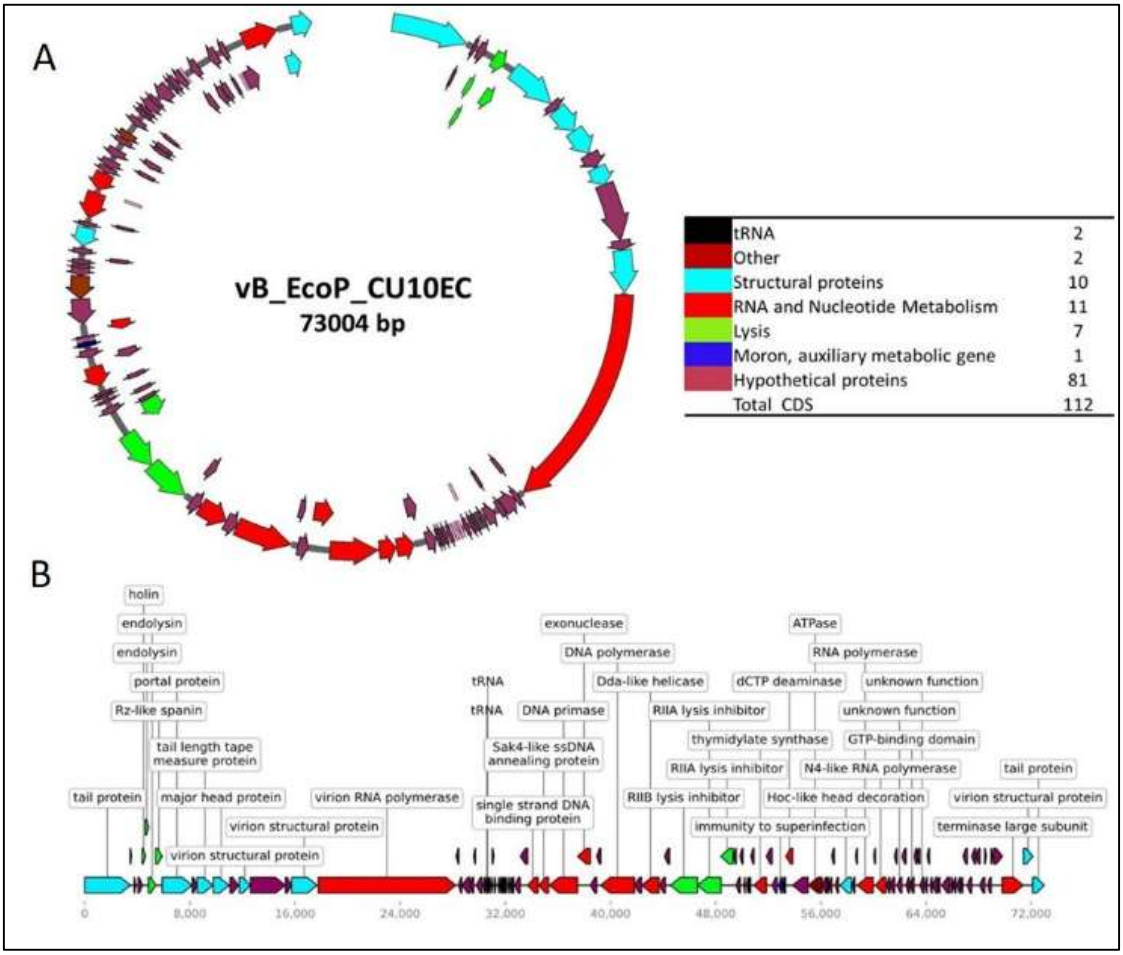


Figure 2. Genomic analysis of CU10EC. (A) Circular genome map of vB_EcoP_CU10EC showing functional annotation. Each block represents a specific functional category, including structural proteins, RNA and DNA metabolism, lysis, auxiliary metabolic genes, tRNAs, other genes, and hypothetical proteins. (B) Linear annotated genome map of Vb_EcoP_CU10EC.

To better understand the phage's genomic profile, taxonomic classification was performed. Taxonomic classification indicated that CU10EC had 72.9% nucleotide similarity to its closest classified phage genome, *Escherichia* phage phi G17 (MH358458). This value is at > 95% species-level threshold, but the < 70% genus-level threshold by TaxMyPhage supports the assignment of CU10EC as a distinct species within the genus *Gamaleyavirus* (Figure 3A). CU10EC belongs to the family of Schitoviridae N4-like phages and the subfamily Enquatrovirinae. Genome annotation also identified an N4-like RNA polymerase (XKC24848.1). A whole-genome-based phylogenetic tree generated using ViPTree placed CU10EC in close relationship with *Escherichia* lytic phage IME11 and other *E. coli* phages (Figure 3B). The CU10EC lifestyle was predicted using PhaTYP, which confirmed its lytic nature (Figure S3).

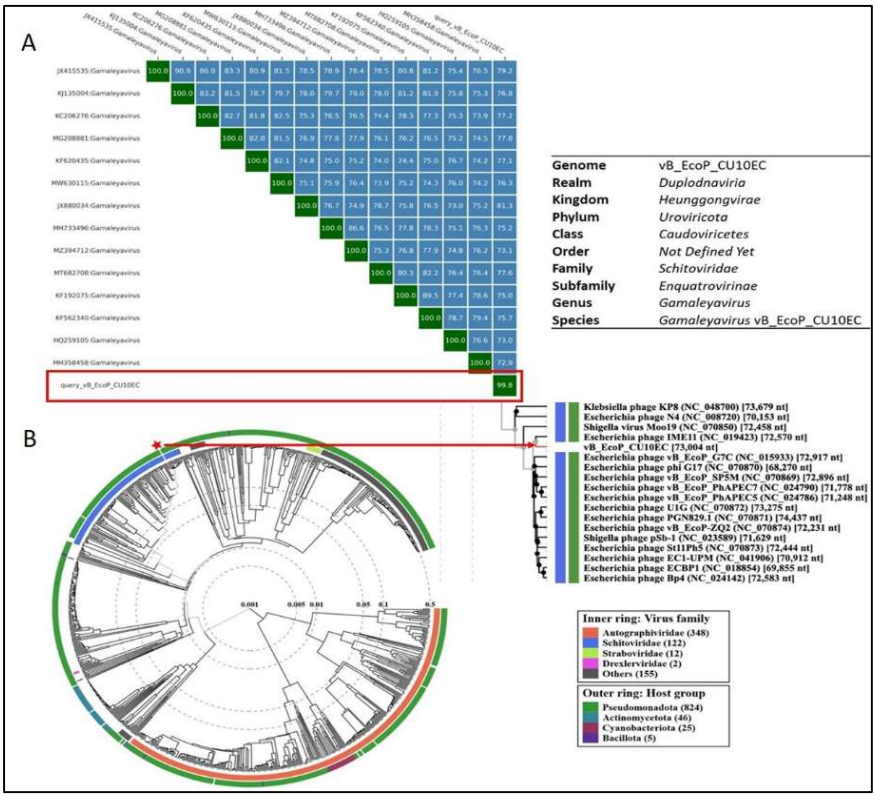


Figure 3. Taxonomic and comparative genomic analysis of CU10EC. (A) ICTV taxonomy of *Escherichia* phage vB_EcoP_CU10EC at the genus and species levels. The phage falls within the genus *Gamaleyavirus* and represents a distinct species, showing 72.9% nucleotide similarity to its closest classified phage genome, *Escherichia* phage phi G17 (MH358458), highlighted in the red box. (B) Proteomic tree of Vb_EcoP_CU10EC alongside closely related *Escherichia* phages. CU10EC is highlighted in red, confirming its place within the family *Schitoviridae*.

3.3. Biological characterization of ETEC phage CU10EC

We conducted a series of experiments to understand the biological characteristics of CU10EC. The host range of CU10EC was assessed using eight *E. coli* strains (Table 1). Among the tested

strains, CU10EC infected and lysed 37.5%, including ETEC MTCC 723 (host), *E. coli* (MG1655), and *E. coli* (TG1) in the spot assay. EOP confirmed that infected strains have a lower EOP value than the host strain. Phage adsorption analysis demonstrated that CU10EC adsorbed approximately 25%–30% within 15 min (Figure 4A). The one-step growth curve revealed a latent period of 20 min, and a burst size corresponding to ~220 PFU/cell (Figure 4B). Stability assays under different physiological conditions indicated that CU10EC remained stable within a pH range of 5–11, with optimal stability observed under neutral to alkaline conditions (Figure 4C). Thermal stability tests revealed that the phage retained high viability between 4 and 40 ℃, while a gradual decline in stability occurred beyond 50 ℃, with complete loss in phage titer at 80 ℃ (Figure 4D). The CU10EC exhibited a strong stability in the presence of bile salt at all three different concentrations without a drop in the titer during experimented time points (Figure S4). The optimum MOI for CU10EC was evaluated using a growth curve assay, with MOI values ranging from 1000 to 0.0001 (Figure S5A). Based on the reduction in bacterial biomass at the lowest MOI, the results showed that an MOI of 1 produced the best reduction by the eighth hour of incubation (Figure S5B). Notably, an increase in biomass was observed after this period, suggesting the rapid emergence of bacterial resistance to the phage. A phage-resistant mutant was isolated for further studies.

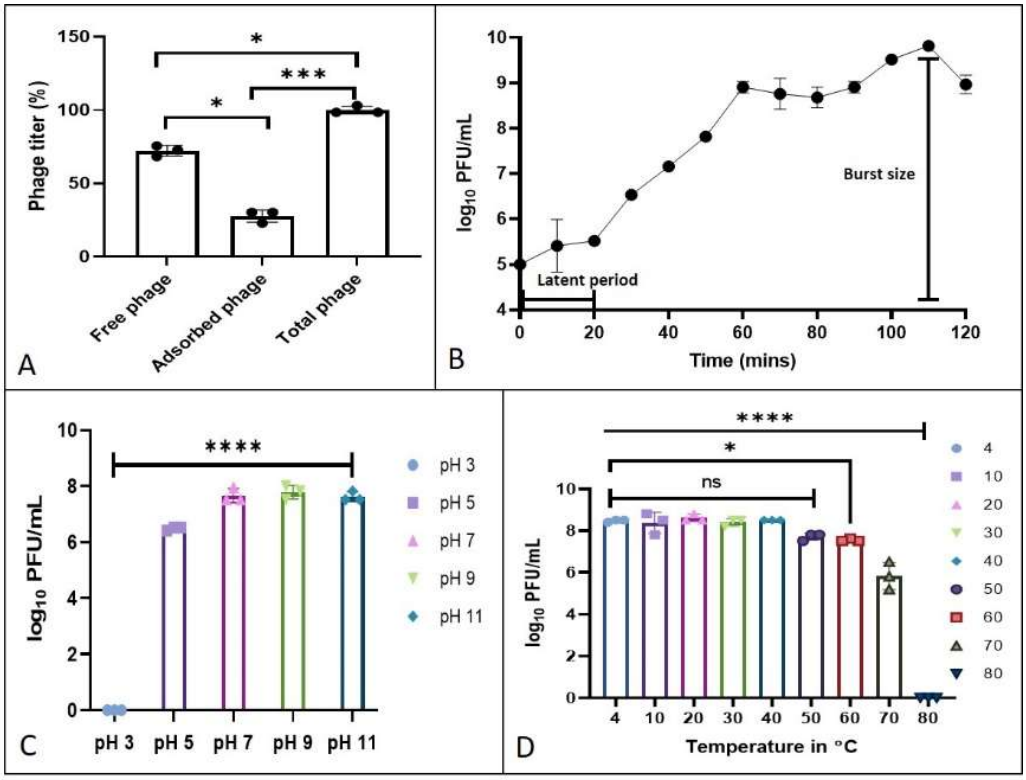


Figure 4. Phage biological characteristics. (A) Adsorption of CU10EC represented in titer percentage. (B) One-step growth curve of CU10EC with a short latent period and maximum burst was observed at the 110th minute. (C–D) Stability of CU10EC in various pH values (3–11) and temperatures (4 to 80 °C). Statistical significance of the groups was determined using an unpaired t-test (A) and one-way ANOVA (C and D) and is indicated as: ns, no significance; * $p \leq 0.05$, ** $p \leq 0.01$; *** $p \leq 0.005$; **** $p \leq 0.0001$. Data were plotted as mean ± SD values of replicates (n = 3).

3.4. Phage-resistant ETEC exhibits altered phenotypic properties compared to wild-type ETEC

The PR-ETEC phenotypic characterization was determined. Resistance was confirmed in both the double-layer agar overlay method and liquid kinetic growth assays. The complete absence of lysis in both agar overlay and liquid media confirmed the host resistance of the PR-ETEC phenotype. A comparative phenotypic study of WT-ETEC and PR-ETEC revealed significant variations in growth and antibiotic susceptibility. WT-ETEC had a shorter lag phase and a faster growth rate, but PR-ETEC produced smaller, slow-growing colonies, indicating poor fitness (Figure 5A,B). Both strains lacked biofilm-forming capability, confirmed by colony patterns on CRA plates. WT-ETEC formed mucoid pale-pink colonies, whereas PR-ETEC produced dry red colonies (Figure 5C). Biofilm quantification determination of WT-ETEC and PR-ETEC using the CV assay revealed that both strains did not produce biofilm, which corroborated with the CRA assay. Antibiotic susceptibility tests revealed that WT-ETEC was resistant to more than three drug classes, indicating MDR status based on standard CLSI breakpoints. In contrast, the ETEC-PR strain exhibited a modified susceptibility pattern. While it maintained resistance to certain core baseline antibiotics, it showed significantly increased zone diameters across several classes compared to the wild type.

Crucially, PR-ETEC displayed newly resolved zones of inhibition for Rifampicin (RIF 5), which was ineffective against ETEC-WT (Figure 5D).

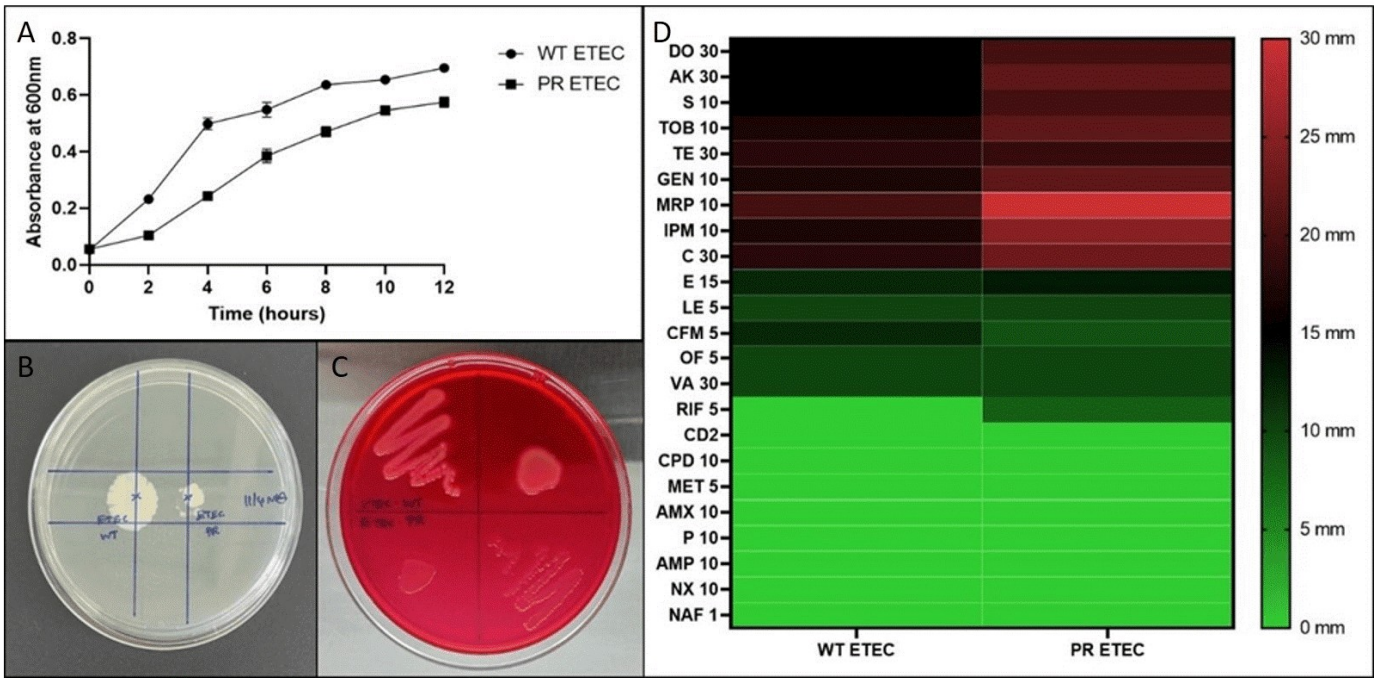


Figure 5. Comparative analysis of WT-ETEC and PR-ETEC. (A) Growth curve analysis in LB broth for 12 h. (B) Colony morphology, motility, and growing pattern of WT-ETEC (left side) and PR-ETEC (right side) on LB agar media. (C) Congo Red Agar assay for analyzing biofilm-forming ability of WT-ETEC (up) and PR-ETEC (down). (D) Anti-biogram of WT-ETEC and PR-ETEC; the zone of inhibition (mm) is presented in a scale bar with different color intensities. Data were plotted as mean ± SD values of replicates (n = 3).

3.5. Composition and antibacterial efficacy of L. acidophilus PB

The PB of *L. acidophilus* was obtained after filter sterilization, and its pH was ~4.6 ± 0.2. Then, heat-processed PB was analyzed using LC-MS to determine its composition. The secretory components of *L. acidophilus* were identified by LC-MS analysis of PB and the modified medium (control). A rigorous chemical matrix subtraction approach using MZmine 3 successfully isolated the authentic cell-free secretome (biogenics) of *L. acidophilus* from the modified medium. Probiotic proliferation and glycolytic activity were validated by a prominent accumulation of lactic acid (m/z 89.06, MSI Level 2). Afterward, the PB had specialized aromatic organic acids, including phenyllactic acid (m/z 166.14, MSI Level 2) and indole-3-lactic acid (m/z 205.24, MSI Level 2), alongside a structurally distinct matrix of microbially metabolized cyclic dipeptides (diketopiperazines), notably Cyclo (Pro-Leu) (m/z 212.19, MSI Level 3) and Cyclo (Phe-Pro) *(*m/z 254.29, MSI Level 3). High-mass envelopes that dominated the late chromatographic profile (m/z 897–1975, ES+) were identified as artifacts from the 0.1% polysorbate (Tween 80) matrix. These signals exhibited a distinct and repeating 44-Da mass differential characteristic of polyoxyethylene surfactant chains, rather than bacterial glycopeptides or plant saponins. Consequently, these non-biological polymer peaks were excluded from the data, restricting the final secretome analysis to true, non-polymeric microbial features (Figure 6 and Table S1).

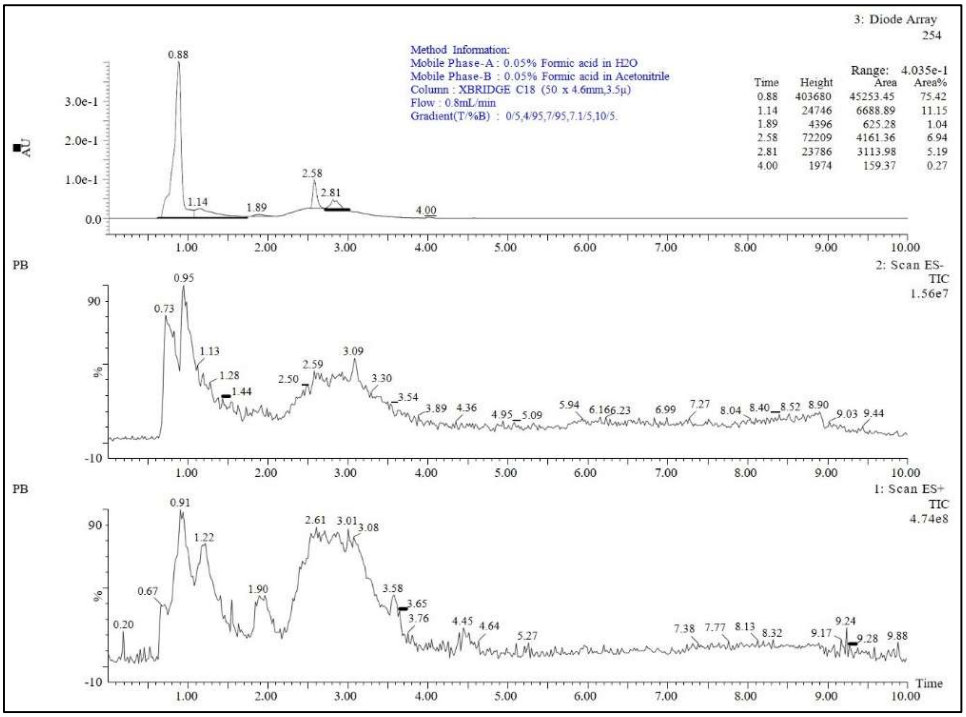


Figure 6. PB characterization. LC-MS total ion chromatogram (TIC) of heat-inactivated PB in positive (ES+) and negative (ES−) ion mode with time, height, and area (%) of compounds present in the sample.

The antibacterial efficacy of the PB was evaluated using well diffusion and MIC assays. In the well diffusion assay, the PB demonstrated significant activity against ETEC, as indicated by pronounced

zones of inhibition (Figure 7A). The MIC assay confirmed that a 25%–30% (v/v) PB concentration effectively inhibited ETEC growth, and the pH was ~5.4 ± 0.2, at which ETEC growth is not inhibited by pH alone, confirming that the effect is due to organic secretory compounds in the PB during incubation. Further assessment using the poison plate method revealed that supplementation of LB medium with 25% PB resulted in the complete suppression of test bacterial growth compared to control plates (Figure 7B). Antimicrobial selectivity assays revealed that the PB displayed selective killing properties, as *L. plantarum* (MTCC-1407), *L. brevis* (MTCC-1750), *L. acidophilus* (MTCC-10307), and *L. salivarius* (MTCC-12829) remained unaffected even at elevated PB concentrations (30%–40%), except *Lactobacillus spp.* (MTCC-4184), which was slightly inhibited at a concentration of 40%.

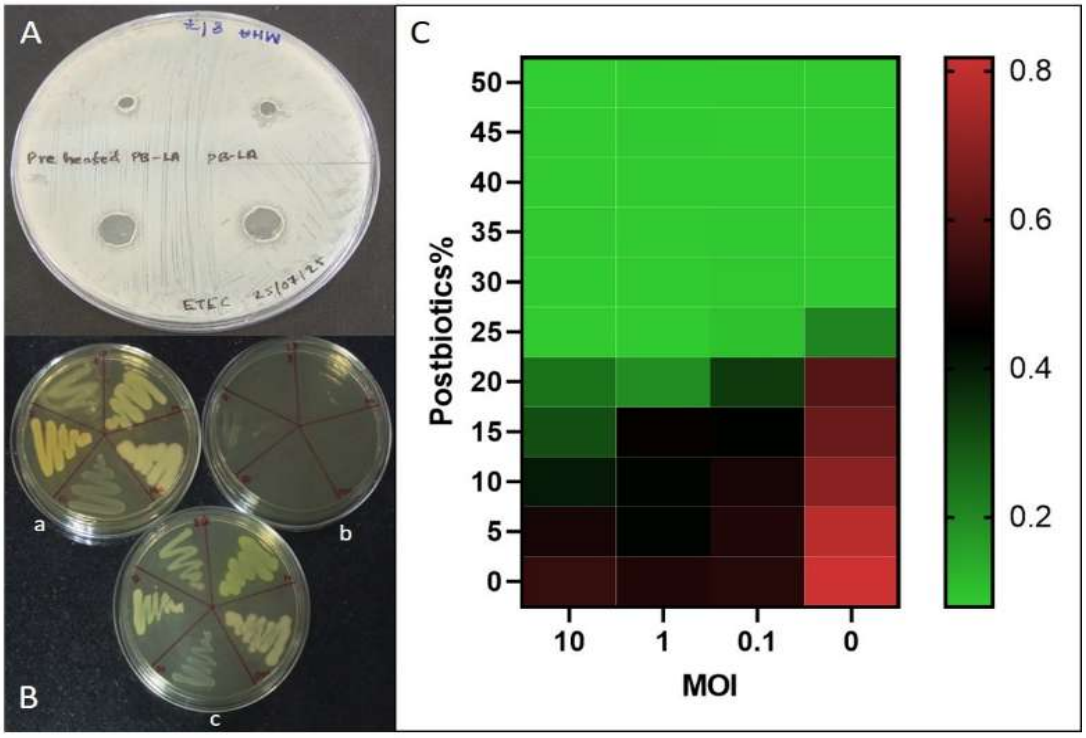


Figure 7. Antimicrobial activities of PB. (A) Well diffusion assay of PB with two different concentrations. (B) PB Poison plate method: a) LP-PB blended plate; b) LA-PB blended plate; c) control LB agar plate without PB. (C) Checkerboard assay for phage-PB combinations against ETEC; the scale bar with different color intensity indicates the absorbance of samples at 600 nm. Data were plotted in mean values of replicates (n = 3).

3.6. Phage-PB combination enhances antibacterial efficacy and delays phage resistance

CU10EC and PB were combined to evaluate their synergistic antibacterial efficacy and potential to reduce the emergence of phage resistance. First, phage stability in PB was assessed, and the phage titer remained stable for up to 24 h. Next, a checkerboard assay was performed to determine the optimal MOI and PB concentration against the MDR ETEC strain (Figure 7C). Among the tested MOIs (10, 1, and 0.1), an MOI of 1 achieved the lowest fractional inhibitory concentration (20%), whereas MOIs of 0.1 and 10 resulted in a minimal inhibitory concentration of 25%. The combination of CU10EC-PB had a Fractional Inhibition Concentration Index (FICI) value of ~0.84.

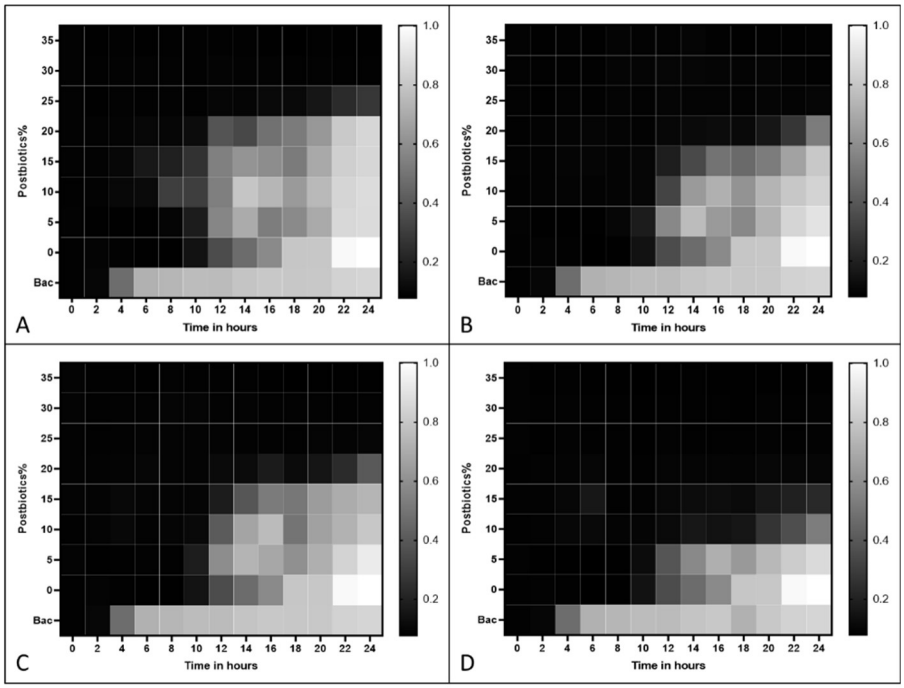


Figure 8. Time-dependent kinetics curve analysis of the phage-PB combination. The bacterial biomass was monitored for all test groups using an OD_{600} at a constant MOI of 1. The Y-axis tracks increasing concentrations of the PB preparation (5%–35%, v/v), including standalone phage treatment (0% PB) and untreated host controls (Bac). The X-axis denotes continuous incubation intervals from 0 to 24 h. The panels represent different staggered treatment timelines: (A) PB co-administered at 0 h (prophylactic treatment). (B) PB administered at the second hour of post-phage infection. (C) PB administered at the fourth hour of post-phage infection. (D) PB administered at the sixth hour of post-phage infection. The scale bar with varying color intensities is provided to validate the biomass values shown in the heatmap. Data were plotted in mean values of replicates (n = 3). Statistical significance was assessed among treatment groups using an RM two-way ANOVA.

The time dependent kinetics curve was then used to evaluate the combined antibacterial activity of CU10EC and PB against ETEC at an MOI of 1. Untreated ETEC controls grew rapidly, while those phage treated at an MOI of 1 induced initial culture clearance, followed by a rapid secondary turbidity rebound starting at the eighth hour. This secondary rebound serves as the operational proxy for the selection and proliferation of a bacteriophage insensitive mutant (BIM) phenotype. PB was administered at four different time points to enhance phage efficacy by delaying the onset of phage resistance. PB addition at the second, fourth, and sixth hours significantly delayed kinetic regrowth by 6–10 h, achieved fractional inhibitory concentrations, and resulted in the lowest biomass compared to prophylactic treatment (Figure 8). Repeated measures (RM) two way ANOVA with a Greenhouse Geisser correction confirmed that the interaction between treatment type and incubation duration was highly significant ($p < 0.0001$). Tukey's post hoc test confirmed that prolonged biomass suppression in the staggered addition cohorts was statistically distinct from both individual therapies and prophylactic combinations ($p < 0.01$).

4. Discussion

The increasing prevalence of MDR ETEC poses a serious global health challenge, necessitating the exploration of alternative antimicrobial strategies beyond conventional antibiotics. Phages are predatory biological entities that can be specifically selected to target pathogenic MDR strains without disturbing commensals, helping control infections in infected individuals and preventing further spread of resistant microbes into the environment [42]. Phage therapy is considered a potential alternative to antibiotics, and for infections like MDR-ETEC, which primarily causes diarrhea, phages can be administered orally or intravenously, depending on the severity of infection. In this regard, the novel lytic bacteriophage, CU10EC, isolated in this study, can be a promising candidate against MDR ETEC. The plaque morphology of CU10EC resembles a bull's-eye type, characterized by a clear center resulting from higher lytic activity and an extending halo caused by the presence of depolymerase, which breaks down the bacterial capsule [43–45].

The genomic analysis confirmed that CU10EC is a strictly lytic phage belonging to the family Schitoviridae. It has structural proteins (head and tail fibers) for genome protection and host adsorption, metabolic proteins that redirect host machinery for phage replication, and lysis proteins (holins, endolysins, spanins) that degrade the bacterial cell envelope to release progeny phages [46,47], lacking genes associated with lysogeny, virulence, or antimicrobial resistance. The taxonomic classification of CU10EC indicates that it belongs to a new species (ANI score < 95%) within the genus *Gamaleyavirus* and the subfamily Enquatrovirinae. The genome annotation reveals that CU10EC encodes an N4-like RNA polymerase (RNAP) with accession number XKC24848.1, a single-polypeptide enzyme (~320 kDa) that facilitates the phage's initiation of the replication cycle immediately after entry into the host bacterial cell [48]. The whole-genome-based phylogenetic tree (ViPTree) of CU10EC confirms that the phage is closely related to lytic phages, such as *Escherichia phage* IME11 and other *Escherichia coli* phages [49,50].

The phage's phenotypic characterizations, including host range, adsorption, one-step growth curve, and stability under various physiological conditions, were analyzed. Host range analysis proved that CU10EC could infect across strains. Spot assays were performed as a preliminary screening of phage susceptible strains. EOP assays were further exploited to determine the phage's lysis efficacy across strains, despite the TG1 strain that showed clear lysis in the spot assay, which had a significantly lower EOP value. These results once again proved that a spot assay may lead to false positive results [51]. Also, no correlation of phage infectivity was observed among the tested strains, regardless of their pathotype. Despite the initial moderate adsorption, CU10EC's propagation increased over time, with a short latent period (~20 min) and a higher burst size (~220 PFU/mL) as determined by the one-step growth curve, compared with previously reported studies [52,53]. Stability across a broad range of pH, temperature, and bile salt concentrations makes CU10EC desirable for gastrointestinal phage therapy applications. CU10EC exhibited strong bile salt stability, in contrast to earlier reports of reduced phage stability [54]. This resistance likely reflects an adaptation to harsh gastrointestinal conditions and is consistent with the findings by Koo et al., who reported bile-resistant *Vibrio* phages targeting enteric bacteria [55].

Although our phage possess superior antibacterial activity, we found that ETEC forms phage-resistant mutants within 10 h against CU10EC. The rapid emergence of phage resistance is a major limitation of phage therapy and has been observed with the majority of phages. Phage resistance is a significant process in phage–bacteria coevolution, in which bacteria employ various adaptations,

driven by mutations at the genotypic level, to survive phage infection. Even in our case, the resistant ETEC mutants have altered growth, reduced fitness, and increased antibiotic susceptibility, which is corroborated by studies showing that phage resistance often involves physiological trade-offs in bacteria. We obtained similar results in our previous study, which involved *P. aeruginosa* (ATCC 15442) and the M12PA phage [26]. Phages that give rise to resistant mutants with altered antibiotic susceptibility are ideal for phage therapy, because their increased antibiotic susceptibility can serve as "Achilles heels" for effective antibiotic synergy. Such a trade-off has been previously reported [16,56,57]. Chan et al. reported that bacterial mutants resistant to the *Pseudomonas* phage OMKO1 became susceptible to multiple antibiotics due to mutations in the efflux pump, which acted as a receptor [58]. In the case of CU10EC, the exact nature of its receptor was not explored. However, based on its high similarity with other N4-like bacteriophages, the receptor is likely to be nfrA and nfrB, whose functions have not been well explored. Notably, in another study, several host mutations unrelated to the receptor have also been shown to confer resistance to N4-like phage infection [59]. Similarly, a zone of inhibition was observed with rifampicin, an antibiotic that kills bacteria by binding to bacterial DNA-dependent RNAP, which blocks the elongation of new RNA transcripts and protein synthesis [60]. Thus, a repertoire of mutations can confer phage resistance, and these phenotypic changes result in a compromised cell membrane, which may allow the antibiotic rifampicin to enter the cell and cause cell death [61].

The efficacy of phage therapy can be improved through combinatorial approaches, including enhancing biofilm penetration, exploiting fitness trade-offs, and reducing the formation of resistance in MDR pathogenic bacteria. A phage-antibiotic combination is the most widely employed method for synergistic action. It has been shown to yield better outcomes than the individual application in treating MDR bacterial infections in *in vitro*, *in vivo*, and clinical settings [26,62]. In previous studies from our lab, we explored compounds with antimicrobial activities that carry a low or no risk of antimicrobial resistance. Specifically, we investigated a combinatorial strategy that combined *Pseudomonas* phage M12PA with green-synthesized AgNPs (*Bauhinia variegata* leaf extract-mediated) against MDR *P. aeruginosa* wound infections, demonstrating promising infection control and wound-healing activity [63]. Other groups have employed various approaches, including combination with probiotics [64], photosensitizers [65], and various nanoparticles [66].

In order to overcome the limitations of phage monotherapy, we investigated a combinatorial approach using a PB derived from *L. acidophilus*. PBs are cell-free supernatants, secretory metabolic components of probiotics, which can contain various elements that help probiotics thrive in their environment. In our study, we utilized known probiotics, including *L. acidophilus*, *L. plantarum*, *L. brevis*, *L. salivarius*, and *L. spp.* All five strains were subjected to physiological stress, including changes in pH and salinity, for PB production. PBs produced at different pH and salinity values were evaluated for their antimicrobial activity. Among the listed bacteria, *L. acidophilus* PB produced in a modified medium at neutral pH (final pH ~4.6 ± 0.2) exhibited a profound antibacterial efficacy against a broad range of MDR pathogens, as determined by a poison plate method and a well diffusion assay. The use of modified medium ensures the antibacterial activity of the PB, which was produced at neutral pH, with less or no toxicity to the host cells and phages. The antibacterial activities of *L. acidophilus*—derived PB have been assessed in several studies against severe foodborne pathogens, such as *E. coli*, *S. typhi*, *S. enterica*, and *Shigella spp.*, having shown convincing antibacterial activity against *P. aeruginosa* and *S. aureus*, as well as modulation of the immune response in *in vivo* wound-healing studies [67,68]. LC-MS revealed that the PB fraction consists of

rich organic, low-molecular-weight metabolites due to active carbohydrate and amino acid metabolism. Notably, the high-mass repeating 44 Da signals were identified as non-biological Tween 80 artifacts and were excluded. Our study demonstrated that the PB exhibits broad antibacterial activity against pathogens due to the presence of phenyllactic acid (PLA) and indole-3-lactic acid (ILA), which are catabolic markers of phenylalanine and tryptophan in PB production. These organic small molecules act as highly stable, membrane-permeabilizing agents that withstand thermal processing without losing structural efficacy, ensuring that the reported antibacterial activity is attributable to metabolites present in the PB. The antibacterial activity of PB was significantly reduced when the PB neutralized to pH 7. This confirms that antibacterial activity in the PB is attributed to organic acids. Selective tolerance toward the tested commensals, while inhibiting the growth of MDR ETEC, is an important consideration for interventions targeting gastroenteritis. Wilsen et al. found that the PB of *L. acidophilus* had a bactericidal effect against *P. aeruginosa* but not against *E. coli,* indicating that *L. acidophilus* secretory products have intrinsic antibacterial activity and species selectivity [69]. However, because our validation was strictly restricted to *in* vitro batch culture using isolated strains, these data support a preliminary hypothesis. The time-based kinetics curve assay revealed the combinatorial benefits of the phage-PB combination against ETEC, with PB exhibiting a fractional inhibitory concentration that delays phage kinetic regrowth and reduces biomass at the second, fourth, and sixth hours of administration. Due to the presence of lactic acid, which lowers the pH and weakens the cell membrane integrity, and the presence of well-documented antibacterial aromatic metabolites, such as PLA and ILA, this duo has shown promising activity against gram-negative pathogens [70,71]. Phage initially infects ETEC, reducing bacterial populations as the primary agent of infection. Subsequent PB administration inhibits mutant regrowth from phage infection, thereby delaying the development of phage resistance and enhancing antibacterial activity. The cyclic dipeptides may be responsible for the delay in regrowth and may support phage action through quorum-sensing interference [71,72]. Notably, the overall biomass of the pathogenic bacteria was significantly reduced at 2, 4, and 6 h of PB administration compared with the prophylactic combination of CU10EC-PB. This time-dependent kinetics assay provides the essential foundation for the *in vivo* validation of infection control in the future.

5. Conclusions

In this work, we investigated the augmentation of the antibacterial properties of the lytic bacteriophage CU10EC, isolated against MDR ETEC, in combination with PB. Phage showed higher lytic activity and infectivity across strains and remained active under a variety of physiologic conditions; whole-genome sequencing confirmed the absence of lysogeny genes, virulence factors, and antibiotic resistance genes. The PB preparations from *L. acidophilus* contained a series of metabolites that enhanced phage antibacterial activity while specifically inhibiting pathogens, without harming commensals. Checkerboard and time-dependent kinetics curve experiments confirmed that the PB and CU10EC combination demonstrated significant antibacterial activity, addressing the major limitation of phage therapy in the treatment system by delaying the emergence of kinetic regrowth (phage resistance) and reducing total biomass. Furthermore, compared with prophylactic therapy, the sequential delivery of phage and PB demonstrated enhanced antibacterial activity. Overall, the combination of phage and PB may provide a reference for a promising alternative therapeutic approach to mitigate prevalent MDR enteric bacterial infections and their spread.

Limitations of the study

The lack of animal model studies for infection control and gut microbiome preservation is a limitation of this study.

Use of AI tools declaration

The authors did not use generative AI tools to create or modify core research data. Assistive AI tools integrated with Word and Google Docs were used to improve language quality.

Acknowledgment

AM, NK, GGX, and KR acknowledge support from the Central University of Tamil Nadu for essential laboratory facilities, ICMR small grant (DDP/10/IIRP-SG2024/00365) and HEFA-CSR grant (SANCSR/05/2025-2026). SG acknowledges support from SRM University AP (SRMAP/URG/GENERAL-D/2025-26/007).

Conflict of interest

None declared.

Author contributions

Abishek Mani: Methodology, data curation, study design, and writing-original draft. Nashath Kalangadan: Methodology, investigation. sharayu magar: methodology, data interpretation, validation. Barath Sivaraj: Methodology, investigation. Gospel Gabriel Xavier: Methodology, investigation. Thirumalai Diraviyam: Resources, visualization. Srivignesh Sundaresan: Formal analysis and visualization. Sutharsan Govindarajan: Resources, supervision, validation, writing-review and editing. Kaushik Rajaram: Conceptualization, supervision, validation, data interpretation, resources, writing-review and editing.

Sequence information

The complete genome sequence of vB_EcoP_CU10EC has been deposited in GenBank under accession number PQ435408.

Data availability statement

The supporting data of this study are available from the Zenodo (Data repository) with the following links, https://doi.org/10.5281/zenodo.23082213 and https://doi.org/10.5281/zenodo.23190352.

References

1. Johura FT, Sultana M, Sadique A, et al. (2024) The antimicrobial resistance of enterotoxigenic *Escherichia coli* from diarrheal patients and the environment in two geographically distinct rural areas in Bangladesh over the years. *Microorganisms* 12: 301. https://doi.org/10.3390/microorganisms12020301
2. World Health Organization (WHO) (2021) WHO Preferred Product Characteristics for Vaccines Against Enterotoxigenic *Escherichia coli*. Available from: https://www.who.int/publications/i/item/who-preferred-product-characteristics-for-vaccines-against-enterotoxigenic-escherichia-coli.
3. Barros MM, Campos AM, Castro J, et al. (2025) An asset for food safety: The knowledge behind the physiological alterations induced by ETEC enterotoxins. *Foods* 14: 3651. https://doi.org/10.3390/foods14213651
4. Qadri F, Svennerholm AM, Faruque ASG, et al. (2005) Enterotoxigenic *Escherichia coli* in developing countries: Epidemiology, microbiology, clinical features, treatment, and prevention. *Clin Microbiol Rev* 18: 465–483. https://doi.org/10.1128/CMR.18.3.465-483.2005
5. Khalil I, Walker R, Porter CK, et al. (2021) Enterotoxigenic *Escherichia coli* (ETEC) vaccines: Priority activities to enable product development, licensure, and global access. *Vaccine* 39: 4266–4277. https://doi.org/10.1016/j.vaccine.2021.04.018
6. Samreen, Ahmad I, Malak HA, et al. (2021) Environmental antimicrobial resistance and its drivers: A potential threat to public health. *J Glob Antimicrob Resist* 27: 101–111. https://doi.org/10.1016/j.jgar.2021.08.001
7. Joffré E, Martín Rodríguez AJ, Justh de Neczpal A, et al. (2025) Emerging multi-drug resistant and extended-spectrum β-lactamase (ESBL)—positive Enterotoxigenic *E. coli* (ETEC) clones circulating in aquatic environments and in patients. *One Health* 20: 100968. https://doi.org/10.1016/j.onehlt.2025.100968
8. Biswas S, Bal M, Pati S, et al. (2024) Antibiotic resistance in toxigenic *E. coli*: A severe threat to global health. *Discov Med* 1: 72. https://doi.org/10.1007/s44337-024-00102-x
9. World Health Organization (WHO) (2025) Bacteriophages and Their Use in Combating Antimicrobial Resistance. Available from: https://www.who.int/europe/news-room/fact-sheets/item/bacteriophages-and-their-use-in-combating-antimicrobial-resistance.
10. Kapoor A, Mudaliar SB, Bhat VG, et al. (2024) Phage therapy: A novel approach against multidrug resistant pathogens. *3 Biotech* 14: 256. https://doi.org/10.1007/s13205-024-04101-8
11. Duan Y, Young R, Schnabl B (2022) Bacteriophages and their potential for treatment of gastrointestinal diseases. *Nat Rev Gastroenterol Hepatol* 19: 135–144. https://doi.org/10.1038/s41575-021-00536-z
12. Khalil IA, Troeger C, Blacker BF, et al. (2018) Morbidity and mortality due to shigella and enterotoxigenic *Escherichia coli* diarrhoea: The Global Burden of Disease Study 1990–2016. *Lancet Infect Dis* 18: 1229–1240. https://doi.org/10.1016/S1473-3099(18)30475-4
13. Sarker SA, Sultana S, Reuteler G, et al. (2016) Oral phage therapy of acute bacterial diarrhea with two coliphage preparations: A randomized trial in children from Bangladesh. *EBioMedicine* 4: 124–137. https://doi.org/10.1016/j.ebiom.2015.12.023

14. Smith WPJ, Wucher BR, Nadell CD, et al. (2023) Bacterial defences: Mechanisms, evolution and antimicrobial resistance. *Nat Rev Microbiol* 21: 519–534. https://doi.org/10.1038/s41579-023-00877-3
15. Berkson JD, Wate CE, Allen GB, et al. (2024) Phage specific immunity impairs efficacy of bacteriophage targeting vancomycin resistant Enterococcus in a murine model. *Nat Commun* 15: 2993. https://doi.org/10.1038/s41467-024-47192-w
16. Mangalea MR, Duerkop BA (2020) Fitness trade offs resulting from bacteriophage resistance potentiate synergistic antibacterial strategies. *Infect Immun* 88: e00926-19. https://doi.org/10.1128/iai.00926-19
17. Kalangadan N, Sundaresan S, Mani A, et al. (2026) Harnessing phage ciprofloxacin synergy to overcome multidrug resistant infections and biofilm persistence. *Arch Microbiol* 208: 663. https://doi.org/10.1007/s00203-026-05223-8
18. Segall AM, Roach DR, Strathdee SA (2019) Stronger together? Perspectives on phage antibiotic synergy in clinical applications of phage therapy. *Curr Opin Microbiol* 51: 46–50. https://doi.org/10.1016/j.mib.2019.03.005
19. Tong Y, Abbas Z, Zhang J, et al. (2025) Antimicrobial activity and mechanism of novel postbiotics against foodborne pathogens. *LWT* 217: 117464. https://doi.org/10.1016/j.lwt.2025.117464
20. El Far MS, Zakaria AS, Kassem MA, et al. (2024) Promising biotherapeutic prospects of different probiotics and their derived postbiotic metabolites: *In vitro* and histopathological investigation. *BMC Microbiol* 23: 122. https://doi.org/10.1186/s12866-023-02866-1
21. D'Carmo Sodré MM, Araújo Cruz ID, Santos UR, et al. (2026) Probiotic cell free supernatants as a strategy against antimicrobial resistance: A systematic review. *Front Cell Infect Microbiol* 16: 1731341. https://doi.org/10.3389/fcimb.2026.1731341
22. Bourebaba Y, Marycz K, Mularczyk M, et al. (2022) Postbiotics as potential new therapeutic agents for metabolic disorders management. *Biomed Pharmacother* 153: 113138. https://doi.org/10.1016/j.biopha.2022.113138
23. Aggarwal S, Sabharwal V, Kaushik P, et al. (2022) Postbiotics: From emerging concept to application. *Front Sustain Food Syst* 6: 887642. https://doi.org/10.3389/fsufs.2022.887642
24. Erdinc AN, Cufaoglu G (2026) Postbiotics as natural antimicrobials: A novel biocontrol strategy for food safety. *Front Bacteriol* 4: 1712139. https://doi.org/10.3389/fbrio.2025.1712139
25. Yaprak Çolak E, Duran N (2025) Synergistic antibacterial effects of postbiotics combined with linezolid and amikacin against nosocomial pathogens. *Front Cell Infect Microbiol* 15: 1616501. https://doi.org/10.3389/fcimb.2025.1616501
26. Mary AS, Kalangadan N, Prakash J, et al. (2024) Relative fitness of wild-type and phage resistant pyomelanogenic *P. aeruginosa* and effects of combinatorial therapy on resistant formation. *Heliyon* 10: e40076. https://doi.org/10.1016/j.heliyon.2024.e40076
27. Bankevich A, Nurk S, Antipov D, et al. (2012) SPAdes: A new genome assembly algorithm and its applications to single cell sequencing. *J Comput Biol* 19: 455–477. https://doi.org/10.1089/cmb.2012.0021
28. Wang RH, Yang S, Liu Z, et al. (2024) PhageScope: A well annotated bacteriophage database with automatic analyses and visualizations. *Nucleic Acids Res* 52: D756–D761. https://doi.org/10.1093/nar/gkad979

29. Bouras G, Nepal R, Houtak G, et al. (2023) Pharokka: A fast scalable bacteriophage annotation tool. *Bioinformatics* 39: btac776. https://doi.org/10.1093/bioinformatics/btac776
30. Wick RR, Schultz MB, Zobel J, et al. (2015) Bandage: Interactive visualization of de novo genome assemblies. *Bioinformatics* 31: 3350–3352. https://doi.org/10.1093/bioinformatics/btv383
31. Shang J, Tang X, Sun Y (2023) PhaTYP: Predicting the lifestyle for bacteriophages using BERT. *Brief Bioinform* 24: bbac487. https://doi.org/10.1093/bib/bbac487
32. Millard A, Denise R, Lestido M, et al. (2025) taxMyPhage: Automated taxonomy of dsDNA phage genomes at the genus and species level. *PHAGE* 6: 5–11. https://doi.org/10.1089/phage.2024.0050
33. Zulkower V, Rosser S (2020) DNA features viewer: A sequence annotation formatting and plotting library for Python. *Bioinformatics* 36: 4350–4352. https://doi.org/10.1093/bioinformatics/btaa213
34. Nishimura Y, Yoshida T, Kuronishi M, et al. (2017) ViPTree: The viral proteomic tree server. *Bioinformatics* 33: 2379–2380. https://doi.org/10.1093/bioinformatics/btx157
35. Wang J, Zhao F, Sun H, et al. (2019) Isolation and characterization of the *Staphylococcus aureus* bacteriophage vB_SauS_SA2. *AIMS Microbiol* 5: 285–307. https://doi.org/10.3934/microbiol.2019.3.285
36. Hu D, Qian P, Gao D, et al. (2024) Characterization and genomics analysis of phage PGX1 against multidrug resistant enterotoxigenic *E. coli* with *in vivo* and *in vitro* efficacy assessment. *Anim Dis* 4: 7. https://doi.org/10.1186/s44149-024-00112-3
37. Ellis EL, Delbrück M (1939) The growth of bacteriophage. *J Gen Physiol* 22: 365–384. https://doi.org/10.1085/jgp.22.3.365
38. Hyman P, Abedon ST (2009) Practical methods for determining phage growth parameters. *Methods Mol Biol* 501: 175–202. https://doi.org/10.1007/978-1-60327-164-6_18
39. Sada TS, Tessema TS (2024) Isolation and characterization of lytic bacteriophages from various sources in Addis Ababa against antimicrobial resistant diarrheagenic *Escherichia coli* strains and evaluation of their therapeutic potential. *BMC Infect Dis* 24: 310. https://doi.org/10.1186/s12879-024-09152-z
40. Clinical and Laboratory Standards Institute (CLSI) (2026) CLSI M100: Performance Standards for Antimicrobial Susceptibility Testing. CLSI. Available from: https://clsi.org/shop/standards/m100/.
41. Basnet A, Tamang B, Shrestha MR, et al. (2023) Assessment of four *in vitro* phenotypic biofilm detection methods in relation to antimicrobial resistance in aerobic clinical bacterial isolates. *PLOS ONE* 18: e0294646. https://doi.org/10.1371/journal.pone.0294646
42. Mafe AN, Büsselberg D (2025) Phage therapy in managing multidrug resistant (MDR) infections in cancer therapy: Innovations, complications, and future directions. *Pharmaceutics* 17: 820. https://doi.org/10.3390/pharmaceutics17070820
43. Asif M, Alvi IA, Waqas M, et al. (2023) A K-17 serotype specific *Klebsiella* phage JKP2 with biofilm reduction potential. *Virus Res* 329: 199107. https://doi.org/10.1016/j.virusres.2023.199107
44. Knecht LE, Veljkovic M, Fieseler L (2020) Diversity and function of phage encoded depolymerases. *Front Microbiol* 10: 2949. https://doi.org/10.3389/fmicb.2019.02949

45. Vukotic G, Obradovic M, Novovic K, et al. (2020) Characterization, antibiofilm, and depolymerizing activity of two phages active on carbapenem resistant *Acinetobacter baumannii*. *Front Med* 7: 426. https://doi.org/10.3389/fmed.2020.00426
46. Young R (2014) Phage lysis: Three steps, three choices, one outcome. *J Microbiol* 52: 243–258. https://doi.org/10.1007/s12275-014-4087-z
47. Guliy OI, Evstigneeva SS (2025) Bacteria- and phage- derived proteins in phage infection. *Front Biosci (Landmark Ed)* 30: 24478. https://doi.org/10.31083/FBL24478
48. Lenneman BR, Rothman Denes LB (2015) Structural and biochemical investigation of bacteriophage N4 encoded RNA polymerases. *Biomolecules* 5: 647–667. https://doi.org/10.3390/biom5020647
49. Fan H, Fan H, An X, et al. (2012) Complete genome sequence of IME11, a new N4-like bacteriophage. *J Virol* 86: 13861. https://doi.org/10.1128/JVI.02684-12
50. Kulikov E, Kropinski AM, Golomidova A, et al. (2012) Isolation and characterization of a novel indigenous intestinal N4-related coliphage vB_EcoP_G7C. *Virology* 426: 93–99. https://doi.org/10.1016/j.virol.2012.01.027
51. Pujato SA, Guglielmotti DM, Martínez García M, et al. (2017) *Leuconostoc mesenteroides* and *Leuconostoc pseudomesenteroides* bacteriophages: Genomics and cross species host ranges. *Int J Food Microbiol* 257: 128–137. https://doi.org/10.1016/j.ijfoodmicro.2017.06.009
52. Dominguez Mirazo M, Harris JD, Demory D, et al. (2024) Accounting for cellular level variation in lysis: Implications for virus-host dynamics. *MBio* 15: e01376-24. https://doi.org/10.1128/mbio.01376-24
53. Acharya S, Chinnasamy T (2025) Therapeutic potential of ECP SA1: A novel lytic phage against multidrug resistant *Escherichia coli*. *Microb Pathog* 208: 107956. https://doi.org/10.1016/j.micpath.2025.107956
54. Yin H, Li J, Huang H, et al. (2021) Microencapsulated phages show prolonged stability in gastrointestinal environments and high therapeutic efficiency to treat *Escherichia coli* O157: H7 infection. *Vet Res* 52: 118. https://doi.org/10.1186/s13567-021-00991-1
55. Koo J, DePaola A, Marshall DL (2000) Effect of simulated gastric fluid and bile on survival of *Vibrio vulnificus* and *Vibrio vulnificus* phage. *J Food Prot* 63: 1665–1669. https://doi.org/10.4315/0362-028x-63.12.1665
56. Fujiki J, Nakamura K, Nakamura T, et al. (2023) Fitness trade offs between phage and antibiotic sensitivity in phage resistant variants: Molecular action and insights into clinical applications for phage therapy. *Int J Mol Sci* 24: 15628. https://doi.org/10.3390/ijms242115628
57. Li N, Zeng Y, Wang M, et al. (2022) Characterization of phage resistance and their impacts on bacterial fitness in *Pseudomonas aeruginosa*. *Microbiol Spectr* 10: e02072–22. https://doi.org/10.1128/spectrum.02072-22
58. Chan BK, Sistrom M, Wertz JE, et al. (2016) Phage selection restores antibiotic sensitivity in MDR *Pseudomonas aeruginosa*. *Sci Rep* 6: 26717. https://doi.org/10.1038/srep26717
59. Mutalik VK, Adler BA, Rishi HS, et al. (2020) High throughput mapping of the phage resistance landscape in *E. coli*. *PLoS Biol* 18: e3000877. https://doi.org/10.1371/journal.pbio.3000877
60. Wehrli W (1983) Rifampin: Mechanisms of action and resistance. *Rev Infect Dis* 5: S407–S411. https://doi.org/10.1093/clinids/5.supplement_3.s407
61. Gomaa SE, Wang Y, Li J, et al. (2025) Phage Henu12-resistant mutant derives fitness trade-offs in *Shigella dysenteriae*. *Microbiol Spectr* 13: e01150-25. https://doi.org/10.1128/spectrum.01150-25

62. Li X, He Y, Wang Z, et al. (2021) A combination therapy of phages and antibiotics: Two is better than one. *Int J Biol Sci* 17: 3573–3582. https://doi.org/10.7150/ijbs.60551
63. Mani A, Shanmugha Mary A, Kalangadan N, et al. (2025) Augmenting phage therapy using green nanotechnology for promising infection control, wound healing and devoiding phage resistance in MDR *Pseudomonas aeruginosa*. *Sci Rep* 15: 30439. https://doi.org/10.1038/s41598-025-00449-w.
64. Choi Y, Kang A, Seo E, et al. (2026) Combination of bacteriophage-probiotics alleviates intestinal barrier dysfunction by regulating gut microbiome in a chick model of multidrug resistant *Salmonella* infection. *J Anim Sci Biotechnol* 17: 14. https://doi.org/10.1186/s40104-025-01324-4
65. Dong S, Shi H, Zhang X, et al. (2018) Difunctional bacteriophage conjugated with photosensitizers for *Candida albicans* targeting photodynamic inactivation. *Int J Nanomedicine* 13: 2199–2216. https://doi.org/10.2147/IJN.S156815
66. Pardo Freire M, Domingo Calap P (2023) Phages and nanotechnology: New insights against multidrug-resistant bacteria. *BioDesign Res* 5: 0004. https://doi.org/10.34133/bdr.0004
67. Rahman MdM, Sazili AQ, Ahmad SA, et al. (2025) Inhibitory efficacy, production dynamics, and characterization of postbiotics of lactic acid bacteria. *BMC Microbiol* 25: 485. https://doi.org/10.1186/s12866-025-04123-z
68. Wilson RM, Walker JM, Beld J, et al. (2025) *Lactobacillus acidophilus* (strain Scav) postbiotic metabolites reduce infection and modulate inflammation in an *in vivo* model of *Pseudomonas aeruginosa* wound infection. *J Appl Microbiol* 136: lxaf061. https://doi.org/10.1093/jambio/lxaf061
69. Wilson RM, Walker JM, Yin K (2021) Different concentrations of *Lactobacillus acidophilus* cell free filtrate have differing anti biofilm and immunomodulatory effects. *Front Cell Infect Microbiol* 11: 737392. https://doi.org/10.3389/fcimb.2021.737392
70. Mani López E, Mejía Garibay B, Hernández Figueroa RH, et al. (2026) Phenyllactic acid from lactic acid bacteria: A natural antimicrobial for food biopreservation. *Fermentation* 12: 184. https://doi.org/10.3390/fermentation12040184
71. Yu J, Hong C, Yin L, et al. (2023) Antimicrobial activity of phenyllactic acid against *Klebsiella pneumoniae* and its effect on cell wall membrane and genomic DNA. *Braz J Microbiol* 54: 3245–3255. https://doi.org/10.1007/s42770-023-01126-8
72. Fernández Garcia L, Blasco L, Bleriot I, et al. (2026) Phages and quorum sensing: Findings to consider in phage therapy. *Eur J Clin Microbiol Infect Dis* 45: 615–629. https://doi.org/10.1007/s10096-025-05375-3



AIMS Press

© 2026 the Author(s), licensee AIMS Press. This is an open access article distributed under the terms of the Creative Commons Attribution License (https://creativecommons.org/licenses/by/4.0)